The University of Sydney

School of Civil Engineering
Sydney NSW 2006
AUSTRALIA

http://www.civil.usyd.edu.au/

Centre for Advanced Structural Engineering

Shear Buckling of Thin-Walled Channel Sections

Research Report No R885

Cao H Pham BE MConstMgt MEngSc
Gregory J Hancock BSc BE PhD DEng

August 2007

ISSN 1833-2781

The University of Sydney

School of Civil Engineering
Centre for Advanced Structural Engineering
http://www.civil.usyd.edu.au/

Shear Buckling of Thin-Walled Channel Sections

Research Report No R885

Cao H Pham, BE, MConstMgt, MEngSc
Gregory J Hancock, BSc, BE, PhD, DEng

August 2007

Abstract:

The elastic buckling stresses of channel sections with and without lips and subject to shear forces parallel with the web are determined where the computational modelling of the thin-walled steel sections is implemented by means of a spline finite strip analysis. Both unlipped and lipped channels are studied where the main variables are the flange width, different boundary conditions and shear flow distribution are considered in this study. The channel sections are also analysed at different lengths to investigate the effect of length/width ratio on the critical shear buckling stresses. Comparisons between cases and with classical solutions are included in this report.

Keywords:

Shear buckling; Thin-walled channel sections; Lipped and unlipped channel sections; Spline finite strip method; Shear buckling capacity; Twisting and lateral buckling mode.

Copyright Notice

School of Civil Engineering, Research Report R885

Email: C.Pham@usyd.edu.au
hancock@eng.usyd.edu.au

ISSN 1833-2781

Published by:
School of Civil Engineering
The University of Sydney
Sydney NSW 2006
AUSTRALIA

August 2007

This report and other Research Reports published by the School of Civil Engineering are available on the Internet:

http://www.civil.usyd.edu.au

TABLE OF CONTENTS

1. INTRODUCTION

Thin-walled sections can be subjected to axial force, bending and shear. In the cases of axial force and bending, the actions causing buckling, either Euler buckling for compression or flexural-torsional buckling for flexure, are well understood. However, for shear, the traditional approach has been to investigate shear plate buckling in the web alone and to ignore the behaviour of the whole section including the flanges. There does not appear to be any consistent investigation of the full section buckling of thin-walled sections under shear. This paper provides solutions to the shear buckling of complete channel sections loaded in pure shear parallel with the web.

The analysis of the shear buckling strength of flat rectangular plates has been performed by many investigators (Timoshenko and Gere, 1961; Bulson, 1970; Bleich, 1952). For a thin flat plate of length *a*, width b_1 and thickness *t* simply supported along all four edges, and loaded by shear stresses distributed uniformly along its four edges, these stresses are equal to the elastic buckling value τ_{cr}, when the plate buckles out of its original plane. The shear buckling stress of an elastic rectangular plate is given by Timoshenko and Gere (1961) as:

$$\tau_{cr} = k_v \frac{\pi^2 E}{12(1-\nu^2)} \left(\frac{t}{b_1}\right)^2 \tag{1}$$

where *E* = modulus of elasticity; ν = Poisson's ratio; b_1 = width of the plate; *t* = thickness of the plate. k_v is the shear buckling coefficient, which depends on the boundary conditions and the aspect ratio of the rectangular plate a/b_1. As the plate is shortened, the number of local buckles is reduced and the value of k_v for a plate simply supported on all four edges is increased from 5.34 for a very long plate to 9.34 for a square plate. An approximate formula for k_v as a function of the aspect ratio of rectangular plate a/b_1 is given as:

$$k = 5.34 + \frac{4}{\left(\frac{a}{b_1}\right)^2} \tag{2}$$

To analyse complete channel sections, the shear buckling analysis is based on a spline finite strip analysis (Lau and Hancock, 1986) implemented by Gabriel Eccher in the program ISFSM Isoparametric Spline Finite Strip Method (Eccher, 2007). Both unlipped and lipped channels of varying section geometry are investigated. Three different methods, which represent different ways of incorporating the shear stresses in the thin-walled section, are used in this paper. These include pure shear in the web only, pure shear in the web and the flanges, and a shear distribution similar to that which occurs in practice allowing for section shear flow. A significant outcome of the study is lateral buckling under shear of sections with narrow flanges. Consequently, sections with and without lateral restraints are studied

2. MODELLING SECTIONS UNDER PURE SHEAR

2.1 Spline Finite Strip Method

The spline finite strip method (Cheung, 1976) is a development of the semi-analytical finite strip method. It uses spline functions in the longitudinal direction in place of the single half sine wave over the length of the section. The advantage of the spline finite strip analysis is that boundary conditons other than simple supports can be easily investigated and buckling in shear is also easily accounted for. The spline finite strip method involves subdividing a thin-walled member into longitudinal strips where each strip is assumed to be free to deform both in its plane (membrane displacements) and out of its plane (flexural displacements). The ends of the section under study are free to deform longitudinally but are prevented from deforming in a cross-sectional plane.

Unlipped Channel

The geometry of the unlipped channel studied is shown in Fig 1. The channel sections consist of a web of width 200 mm, a flange of width 0.01 mm to 160 mm, both with thickness of 2 mm. The member is subdivided into 36 longitudinal strips which include 16 strips in the web and 10 strips in each flange. The lengths of the member studied are 1000 mm and 200 mm. The aspect ratios of the web rectangular plate are therefore $b_1/a = 0.2$ and $b_1/a = 1.0$ respectively.

Lipped Channel

The geometry of the lipped channel studied is shown in Fig 2. The channel section consists of a web of width 200 mm, a flange of width 0.01 mm to 160 mm, a lip size of 20 mm, all with thickness 2 mm. The member is subdivided into 40 longitudinal strips which include 16 strips in the web, 10 strips in each flange and 2 strips in each lip. The lengths of the member studied are 1000 mm and 200 mm. The aspect ratios of the web rectangular plate are therefore $b_1/a = 0.2$ and $b_1/a = 1.0$ respectively.

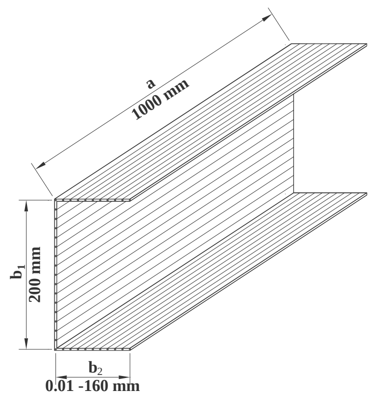

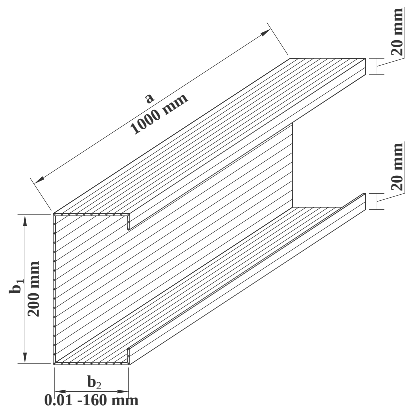

Figure 1. Unlipped Channel Geometry Figure 2. Lipped Channel Geometry

2.2 Shear Stress Distribution

In order to demonstrate the different ways in which a channel member may buckle under shear stress, four cases of shear stress distribution are investigated. In *Cases A* and *B*, uniform pure shear stress is applied throughout the web panel as shown in Fig 3(a), 4(a). The only difference between *Case A* and *B* is that two longitudinal edges of the channel member in *Case A* are restrained laterally whereas there is no restraint along the two longitudinal edges in *Case B*. In *Case C*, the pure shear stress is uniform in both the web and the flanges as shown in Fig 3(b), 4(b). Although this case is unrealistic in practice, it investigates the effect of the flanges on the buckling of the member under pure shear stress. *Case D* models the case which occurs in practice namely, a shear flow distribution as shown in Fig 3(c), 4(c) resulting from a shear force parallel with the web. To simulate the variation in shear stress, each strip in the cross-section is assumed to be subjected to a pure shear stress which varies from one strip to the other strip. The more the cross-section is subdivided into strips, the more accurately the shear stress is represented in order to match the practical shear flow distribution.

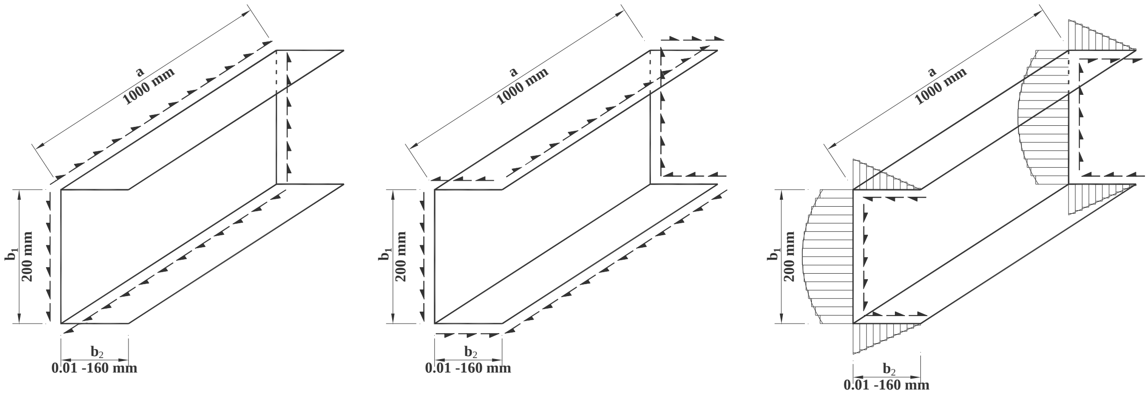

(a) <u>Case A & Case B</u> *(b) <u>Case C</u>* *(c) <u>Case D</u>*

Figure 3. Shear Flow Distribution in Unlipped Channel

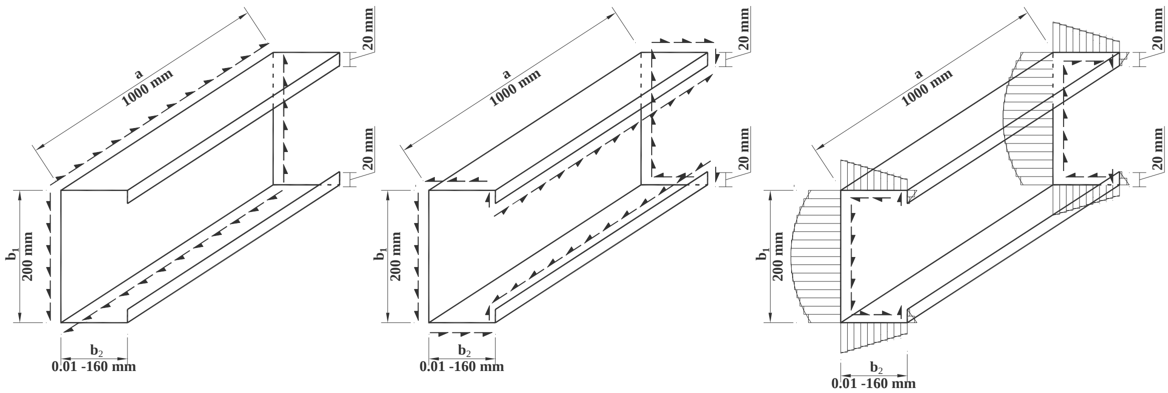

(a) <u>Case A & Case B</u> *(b) <u>Case C</u>* *(c) <u>Case D</u>*

Figure 4. Shear Flow Distribution in Lipped Channel

2.3 Lateral Restraints and Boundary Conditions

Two types of boundary conditions are used for the analysis of all cases in this report. A combination of lateral restraints along the two longitudinal edges of web panels and simply supported edges of the end cross-section plane is applied in *Case A*. In the remaining cases *(Cases B,C & D)*, there are no lateral restraints along the two longitudinal edges of web panels. All edges of the end cross-section are simply supported. Fig 5 and Table 1 show the lateral restraints and boundary conditions of the unlipped channel. Fig 6 and Table 2 show those for the lipped channel.

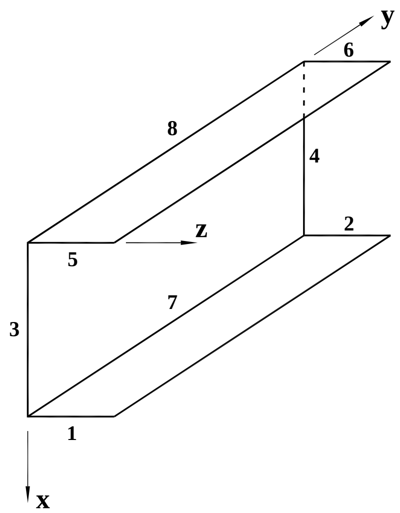

Figure 5

Cases	Edges	*u*	*v*	*w*
A	1 2 5 6 3 4 7 8	1 0	0 0	0 1
B,C & D	1 2 5 6 3 4 7 8	1 0 0	0 0 0	0 1 0
Note: *u, v* and *w* are translations in the *x,y* and *z* directions respectively. 0 denotes free and 1 denotes restraint DOF				

Table 1. Boundary Conditions of Unlipped Channel

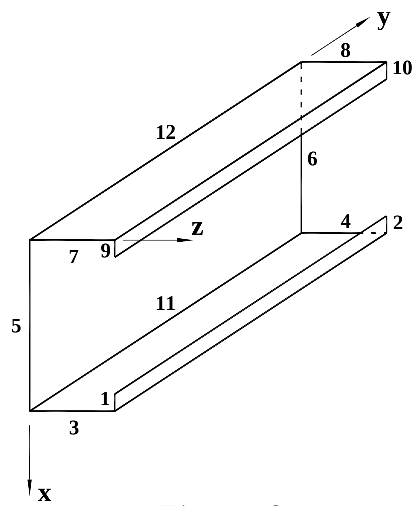

Figure 6

Cases	Edges	*u*	*v*	*w*
A	3 4 7 8 1 2 5 6 9 10 11 12	1 0	0 0	0 1
B,C & D	3 4 7 8 1 2 5 6 9 10 11 12	1 0 0	0 0 0	0 1 0
Note: *u, v* and *w* are translations in the *x,y* and *z* directions respectively. 0 denotes free and 1 denotes restraint DOF				

Table 2. Boundary Conditions of Lipped Channel

3. RESULTS OF BUCKLING ANALYSES

3.1 Unlipped Channel Section – Length = 1000 mm, b_1/a = 0.2

Section	b_2/b_1	Case A Buckling Stress (MPa)	Case A k_v	Case B Buckling Stress (MPa)	Case B k_v	Case C Buckling Stress (MPa)	Case C k_v	Case D Buckling Stress (MPa)	Case D k_v
200x0.01	0.00005	99.603	5.510	1.965	0.109	1.965	0.109	1.966	0.109
200x5	0.025	101.072	5.591	3.315	0.183	3.315	0.183	3.310	0.183
200x10	0.05	102.936	5.695	10.479	0.580	10.477	0.580	10.434	0.577
200x15	0.075	104.688	5.791	21.333	1.180	21.271	1.177	21.721	1.202
200x20	0.1	106.332	5.882	31.024	1.716	30.799	1.704	31.532	1.744
200x40	0.2	111.922	6.192	72.415	4.006	69.537	3.847	70.485	3.899
200x60	0.3	116.138	6.425	105.803	5.853	96.219	5.323	98.372	5.442
200x80	0.4	119.240	6.596	118.100	6.533	93.982	5.199	106.974	5.918
200x100	0.5	121.464	6.720	120.811	6.683	73.607	4.072	109.965	6.083
200x120	0.6	123.020	6.806	122.565	6.780	55.702	3.081	111.250	6.155
200x140	0.7	124.090	6.865	123.739	6.845	43.273	2.394	110.958	6.138
200x160	0.8	124.817	6.905	124.526	6.889	34.362	1.901	108.735	6.015

Table 3. Buckling Stress and The Shear Buckling Coefficients *(k_v)* of Unlipped Channel Section

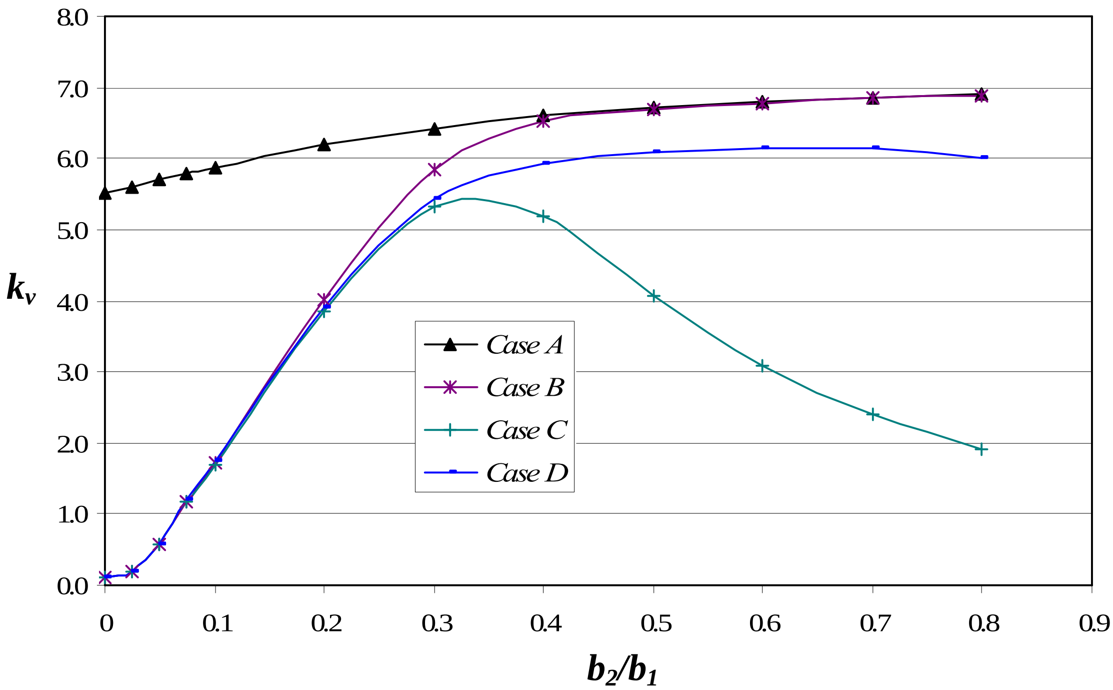

Figure 7. The Ratio of Flange and Web Widths *(b_2/b_1)* and The Shear Buckling Coefficients *(k_v)*

The results of the bucking analyses of the unlipped channel section with a length of 1000 mm are shown in Table 3 and Fig 7 for the ratios of flange to web widths *(b_2/b_1)* from 0.00005 to 0.8. The buckling stresses and the shear buckling coefficients *(k_v)* of all *Cases (A,B,C & D)* are also included in this table. The corresponding buckling modes are shown in Fig 8.

As can be seen in Fig 7 which illustrates the relation between the ratio of flange and web widths *(b_2/b_1)* and the shear buckling coefficients *(k_v)*, when the flange width is very small (0.01 mm), the value of k_v for *Case A* with lateral restraint is 5.51 which is very close to the theoretical result (Timoshenko and Gere, 1961; Bulson, 1970; Bleich, 1952). As the flange width increases, the value of k_v increases as a result of the elastic torsional restraint of the flange on the web. However, for *Case B*, the shear flow applied is similar to *Case A* with no lateral restraints along the two longitudinal edges of web panel. It can be seen in Fig 7 and Fig 8 that the channel member buckles sideways for the ratio of b_2/b_1 of 0.00005 and the value of k_v is then very close to zero (0.109). The value of k_v increases slightly to 0.183 when the ratio of b_2/b_1 is 0.025. It is interesting to note that when the ratio of b_2/b_1 increases from 0.025 to around 0.3, the value of k_v increases dramatically from 0.183 to 5.853. Fig 8 shows the twisting buckling mode shape in the cases of the ratio of b_2/b_1 from 0.025 to 0.3. As the ratio of b_2/b_1 keeps increasing to 0.4, the value of k_v still improves but the increment reduces. Finally, the curve matches with that of *Case A.* The explanation is due to the fact that there is apparently more lateral and torsional restraint being provided by the flange.

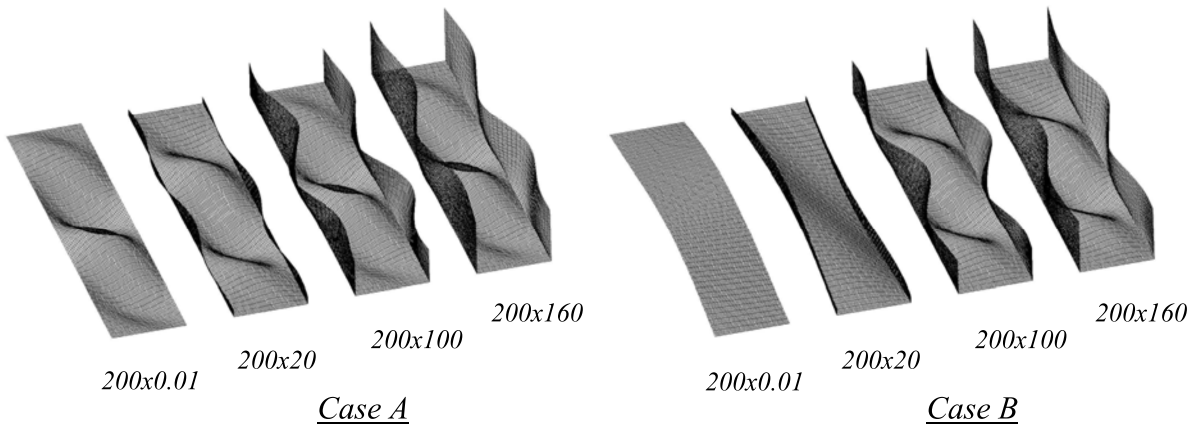

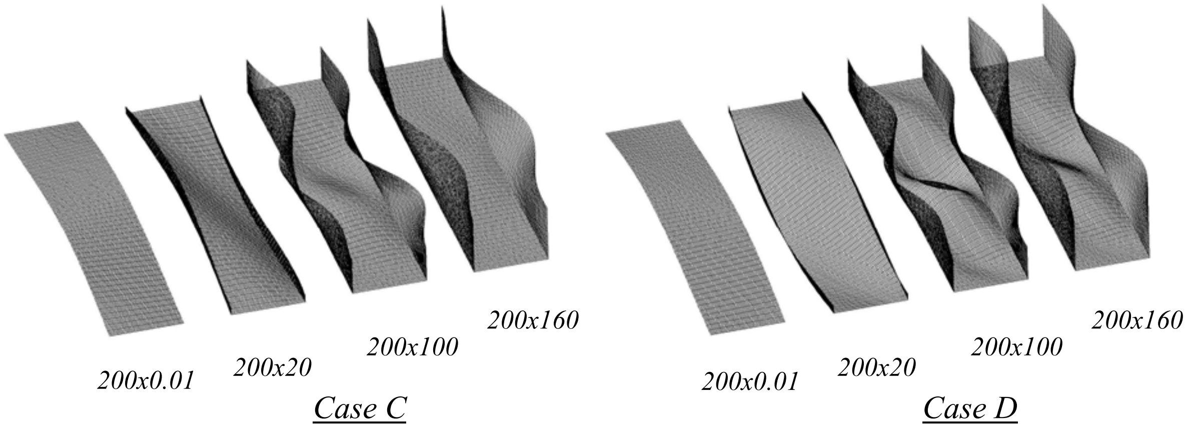

Figure 8. Buckling Mode Shape of Unlipped Section – Length = 1000 mm, $b_2/a = 0.2$

It can be seen in Fig 7 that in *Case C* with pure shear flow applied in the web and the flange and in *Case D* with actual shear flow applied, when the flange width is small (from 0.01mm to 40mm), the values of k_v are not significantly different from that of *Case B*. However, from the ratio of b_2/b_1 of 0.4 the value of k_v for *Case C* reduces dramatically whereas the value of k_v for *Case D* still increases but are below that of *Case B.* The explanation is mainly a result of the effect of shear stresses in the flanges.

3.2 Lipped Channel Section – Length = 1000 mm, $b_1/a = 0.2$

Section	b_2/b_1	*Case A*		*Case B*		*Case C*		*Case D*	
		Buckling Stress (MPa)	k_v	Buckling Stress (MPa)	k_v	Buckling Stress (MPa)	k_v	Buckling Stress (MPa)	k_v
200x0.01x20	0.00005	106.370	5.885	2.363	0.131	2.915	0.161	2.349	0.130
200x5x20	0.025	111.791	6.184	13.950	0.772	16.672	0.922	13.724	0.759
200x10x20	0.05	121.327	6.712	27.841	1.540	34.436	1.905	28.110	1.555
200x15x20	0.075	130.441	7.216	41.338	2.287	49.896	2.760	41.234	2.281
200x20x20	0.1	136.668	7.561	55.185	3.053	64.570	3.572	54.153	2.996
200x40x20	0.2	139.021	7.691	109.082	6.035	113.316	6.269	101.054	5.590
200x60x20	0.3	135.454	7.493	133.336	7.376	132.631	7.337	119.021	6.584
200x80x20	0.4	132.683	7.340	131.654	7.283	130.722	7.232	119.440	6.608
200x100x20	0.5	130.749	7.233	130.129	7.199	128.335	7.100	119.440	6.608
200x120x20	0.6	129.416	7.159	128.985	7.136	121.320	6.712	119.337	6.602
200x140x20	0.7	128.495	7.109	128.163	7.090	97.709	5.405	119.116	6.590
200x160x20	0.8	127.857	7.073	127.581	7.058	78.997	4.370	118.734	6.569

Table 4. Buckling Stress and The Shear Buckling Coefficients *(k_v)* of Lipped Channel

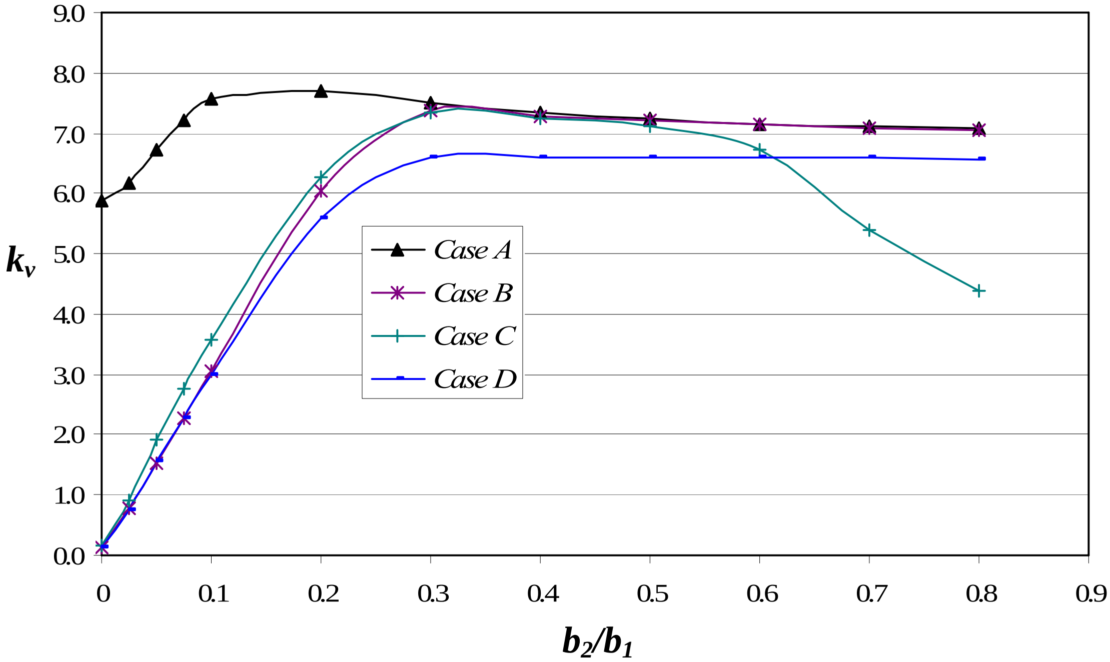

Figure 9. The Ratio of Flange and Web Widths *(b_2/b_1)* and The Shear Buckling Coefficients *(k_v)*

Table 4 and Fig 9 show the results of the buckling analyses of the lipped channel section with a length of 1000 mm and the ratios of flange to web width *(b_2/b_1)* from 0.00005 to 0.8. The lip size of 20 mm is used throughout the analyses. The corresponding buckling mode shapes are shown in Fig 10.

Fig 9 shows the relationship between the ratio of flange and web width *(b_2/b_1)* and the shear buckling coefficients *(k_v)*. As the ratio of b_2/b_1 is small (0.00005), the value of k_v for *Case A* with lateral restraint is 5.885 which is slightly higher than that of *Case A* in Section 3.1. The reason is due to the presence of two lips which improves the shear capacity of the channel section member. As the ratio of b_2/b_1 increases to 0.1, the value of k_v goes up rapidly. The explanation is that the small flange width with the lip contributes significantly to shear buckling capacity of the lipped channel section. It should be noted that when the ratio of b_2/b_1 increases from 0.1 to 0.2, the value of k_v improves slowly from 7.561 to 7.691 respectively. The value of k_v then reduces to 7.073 as the flange width increases to 0.8. The explanation for this fact is due to the effect of flange slenderness. As the flange width is small, there is little or no effect of flange slenderness on the shear buckling capacity. However, when flange width increases, the effect of flange slenderness is quite considerable.

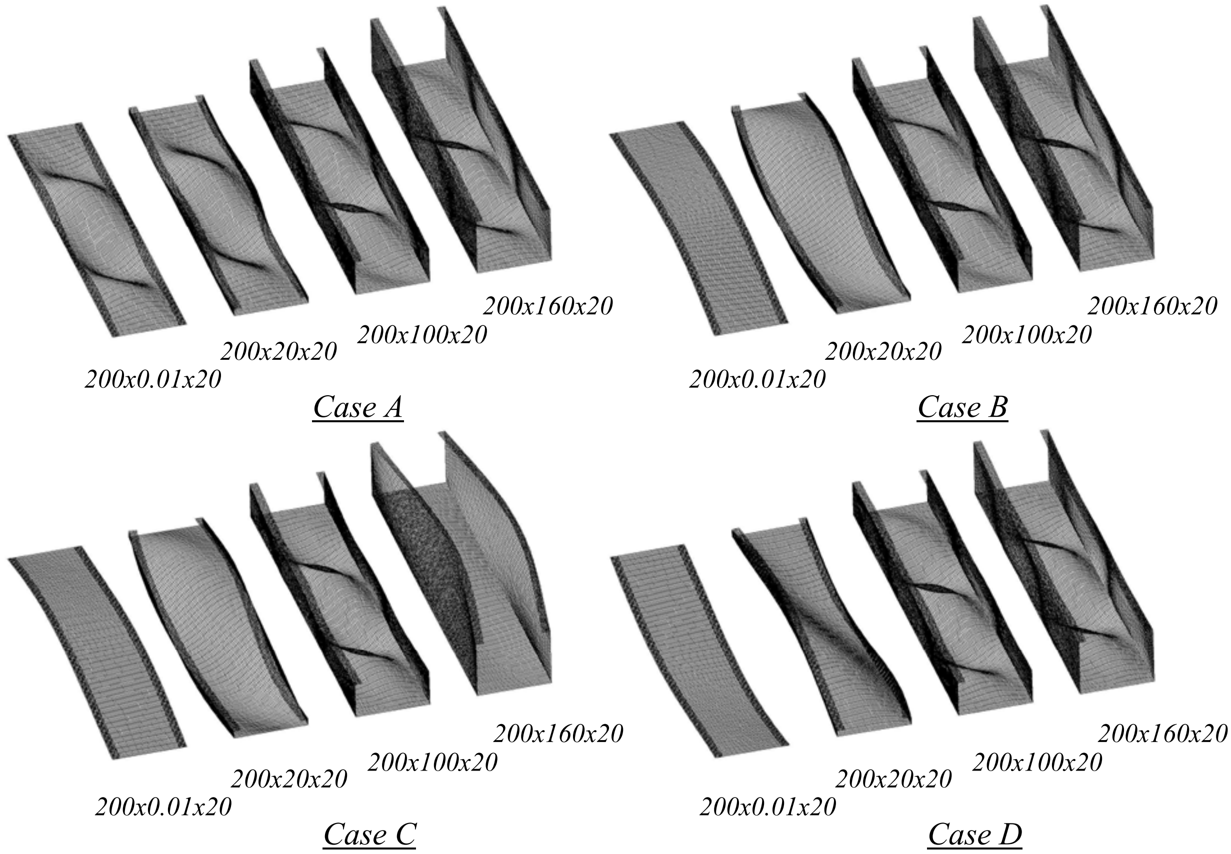

Figure 10. Buckling Mode Shape of Lipped Section – Length = 1000 mm, $b_2/a = 0.2$

It can be seen in Fig 9 that without lateral restraints along two longitudinal edges of the web panel when the ratio of b_2/b_1 is 0.01, the values of k_v for *Case B* and *C* are quite small (0.131 and 0.161 respectively). Fig 10 shows that the lipped channel members of *Case B* and *C* buckle sideways. When the ratio of b_2/b_1 increases from 0.01 to 0.3, the values of k_v for *Case B* and *C* also increase to 7.376 and 7.337 respectively which are higher than those of the unlipped channel section in Section 3.1 due to the presence of the lips. As can be seen in Fig 10, the buckling mode shapes are twisting modes. This can be explained that the flanges with lips affect partly on the lateral restraints along two longitudinal edges of the web panel.

As the ratio of b_2/b_1 increases to 0.3, the k_v curves of *Case B* and *C* nearly match with that of *Case A.* The flanges with lips are long enough to give full lateral restraints to the lipped channel section members. While the values of k_v for *Case B* are very close to that of *Case A* as the ratio of b_2/b_1 increases from 0.3 to 0.8 , the value of k_v for *Case C* reduces when the ratio of b_2/b_1 is in the range 0.5 to 0.8. The reason is that *Case C* with pure shear flow applied in both the web and the flange buckles in the flanges as well as the web and the lips buckle sideways.

In *Case D* with actual shear flow applied, the relation curve between the ratio b_2/b_1 and the value of k_v is similar to that of *Case B*. As the ratio of b_2/b_1 increases from 0.01 to 0.4, the value of k_v increases rapidly from 0.130 to 6.608. From the ratio of b_2/b_1 of 0.4, the value of k_v reduces slightly to 6.569. As can be seen in Fig 10, the k_v curve of *Case D* is below that of *Case A*. This is apparently due to the effect of the shear stress developed in the flanges. However, the lips do not buckle sideways as for *Case C*.

3.3 Unlipped Channel Section – Length = 200 mm, b_1/a = 1.0

Section	b_2/b_1	*Case A*		*Case B*		*Case C*		*Case D*	
		Buckling Stress (MPa)	k_v	Buckling Stress (MPa)	k_v	Buckling Stress (MPa)	k_v	Buckling Stress (MPa)	k_v
200x0.01	0.00005	167.111	9.245	75.750	4.191	75.750	4.190	79.854	4.418
200x5	0.025	170.386	9.426	115.742	6.403	115.696	6.400	110.790	6.129
200x10	0.05	174.201	9.637	164.038	9.075	163.942	9.069	134.194	7.424
200x15	0.075	177.452	9.817	173.080	9.575	173.017	9.572	142.032	7.857
200x20	0.1	180.206	9.969	177.745	9.833	177.768	9.834	147.531	8.162
200x40	0.2	187.489	10.372	186.599	10.323	186.981	10.344	161.939	8.959
200x60	0.3	191.091	10.571	190.417	10.534	190.015	10.512	170.424	9.428
200x80	0.4	192.910	10.672	192.298	10.638	171.895	9.509	175.708	9.720
200x100	0.5	193.865	10.725	193.280	10.693	133.935	7.409	179.060	9.906
200x120	0.6	194.384	10.754	193.816	10.722	111.707	6.180	181.211	10.025
200x140	0.7	194.672	10.770	194.117	10.739	97.847	5.413	182.582	10.101
200x160	0.8	194.831	10.778	194.286	10.748	88.480	4.895	183.411	10.147

Table 5. Buckling Stress and The Shear Buckling Coefficients *(k_v)* of Unlipped Channel

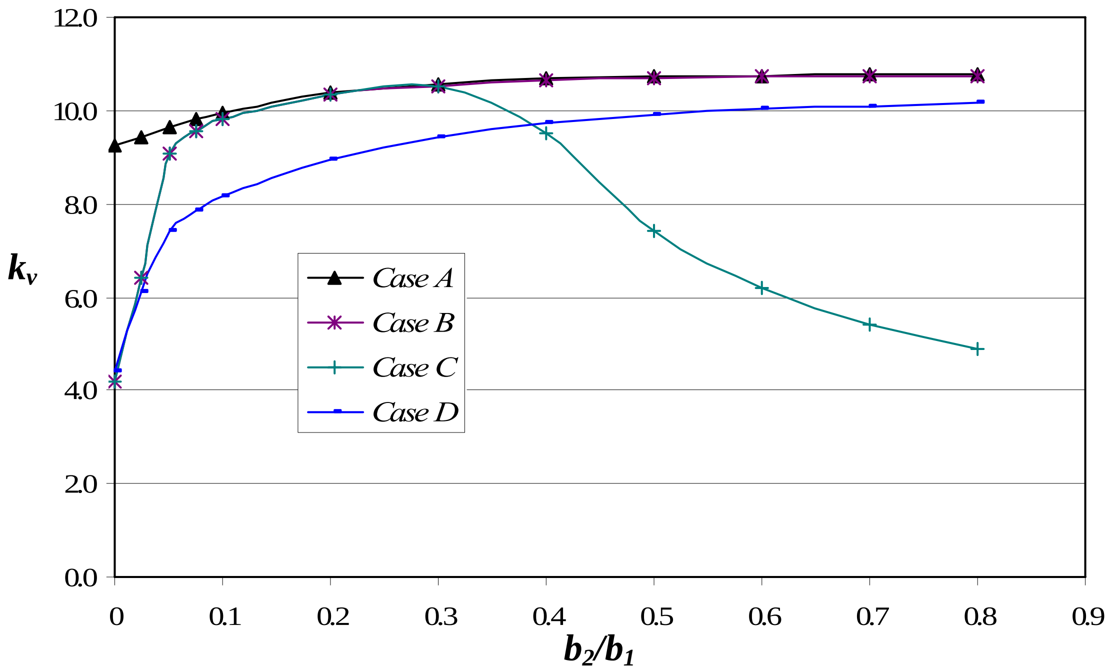

Figure 11. The Ratio of Flange and Web Widths *(b_2/b_1)* and The Shear Buckling Coefficients *(k_v)*

The results of the bucking analyses of the unlipped channel section with a length of 200 mm are shown in Table 5 and Fig 11. Table 5 includes different channel sections, the ratios of flange and web width *(b_2/b_1)*, the buckling stresses and the shear buckling coefficients *(k_v)* of all *Cases (A,B,C & D)*. The relationships between the ratio of flange and web width *(b_2/b_1)* and the shear buckling coefficient *(k_v)* for all four cases are plotted in Fig 11. The corresponding buckling mode shapes are shown in Fig 12.

It can be seen in Table 5 that when the ratio of b_1/b_2 is 0.00005, the value of k_v for *Case A* with lateral restraints along edges of web panel is 9.245 which is close to the theoretical value (Timoshenko and Gere, 1961; Bulson, 1970; Bleich, 1952). As the ratio of b_2/b_1 increases to 0.8, the value of k_v increases to 10.778. The shear buckling capacity is therefore improved as the flange width increases.

At the ratio of b_2/b_1 of 0.00005, the values of k_v for *Case B, C* and *D* with no lateral restraints are 4.191, 4.190 and 4.418. These values are significantly higher than those of the unlipped channel member of 1000 mm length in Section 3.1. It is interesting to note that with greater ratio between the web width and member length *(b_1/a)* the value of k_v is significantly greater than 0.0 even for very small flange widths. It can also be seen in Fig 12 the buckling mode shapes of these cases are both sideways and twisting.

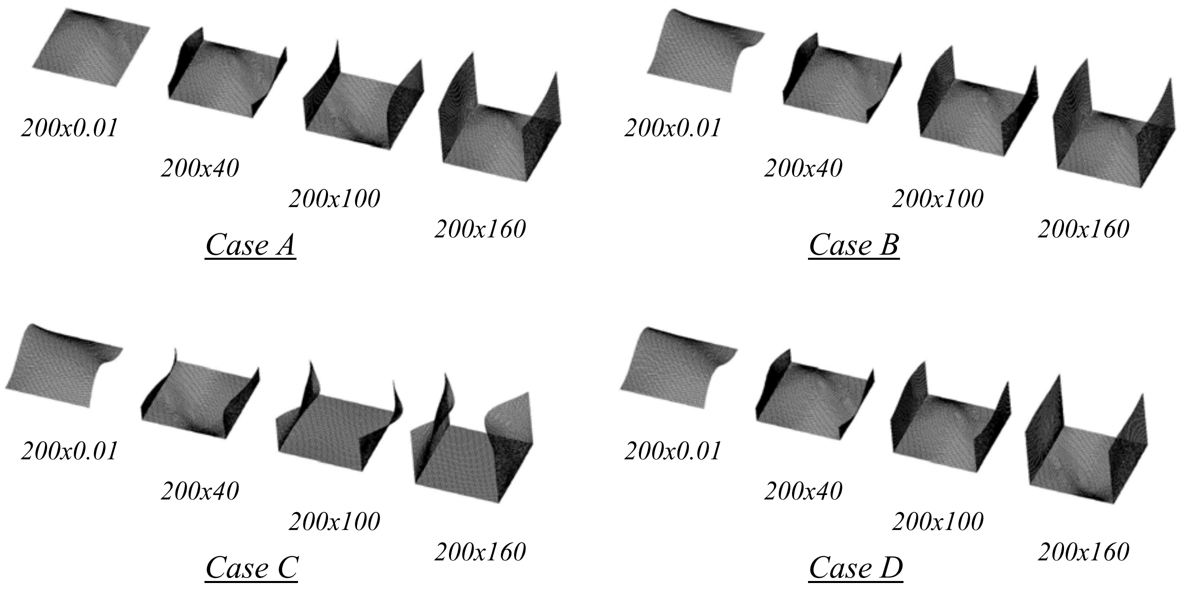

Figure 12. Buckling Mode Shape of Unlipped Section – Length = 200 mm, b_2/a = 1.0

For small increment of the ratio of b_2/b_1 from 0.00005 to 0.05, the values of k_v for *Case B* and *C* increase dramatically to 9.075 and 9.069. As the ratio of b_2/b_1 keeps increasing to 0.1, the k_v curves for these cases are close and start matching with that of *Case A.* It can be seen that the ratio of b_2/b_1 only needs to increase to 0.1 to get full lateral restraint, whereas for the 1000 mm length unlipped channel section member in Section 3.1 the ratio of b_2/b_1 needed to increase to 0.3 to achieve the same effect. Similar to *Case C* in Section 3.1, the value of k_v reduces when the ratio of b_2/b_1 increases from 0.3 to 0.8 due to shear buckling which mainly occurs in the flanges. In *Case D* with the actual shear flow applied, the increment of the value of k_v is quite similar to that of *Case B.* However, the k_v curve of *Case D* is lower than that of *Case B*.The explanation is that there is gradual shear flow distributed in the flange and the shear flow in the web is parabolic instead of pure shear as in *Case B.*

3.4 Lipped Channel Section – Length = 200 mm, b_1/a = 1.0

Section	b_2/b_1	Case A		Case B		Case C		Case D	
		Buckling Stress (MPa)	k_v	Buckling Stress (MPa)	k_v	Buckling Stress (MPa)	k_v	Buckling Stress (MPa)	k_v
200x0.01x20	0.00005	180.273	9.973	94.148	5.208	99.713	5.516	92.735	5.130
200x5x20	0.025	194.069	10.736	166.975	9.237	169.337	9.368	137.805	7.624
200x10x20	0.05	203.498	11.258	188.970	10.454	189.524	10.485	154.758	8.561
200x15x20	0.075	206.220	11.408	198.663	10.990	198.822	10.999	164.369	9.093
200x20x20	0.1	206.409	11.419	202.172	11.184	202.295	11.191	169.483	9.376
200x40x20	0.2	202.658	11.211	201.719	11.159	201.845	11.166	175.956	9.734
200x60x20	0.3	199.598	11.042	199.098	11.014	199.107	11.015	177.964	9.845
200x80x20	0.4	197.783	10.942	197.382	10.919	197.226	10.911	179.450	9.927
200x100x20	0.5	196.728	10.883	196.352	10.862	195.948	10.840	180.797	10.002
200x120x20	0.6	196.101	10.849	195.731	10.828	194.911	10.783	182.016	10.069
200x140x20	0.7	195.717	10.827	195.346	10.807	193.764	10.719	183.063	10.127
200x160x20	0.8	195.471	10.814	195.099	10.793	191.913	10.617	184.165	10.188

Table 6. Buckling Stress and The Shear Buckling Coefficients *(k_v)* of Lipped Channel

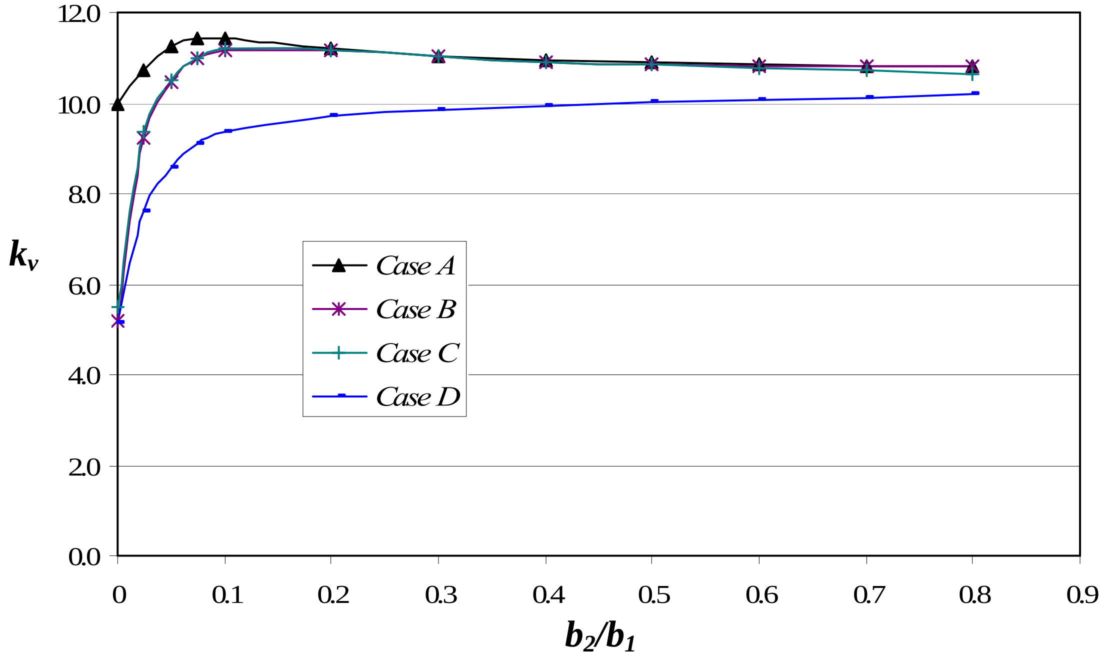

Figure 13. The Ratio of Flange and Web Widths *(b_2/b_1)* and The Shear Buckling Coefficients *(k_v)*

Table 6 and Fig 13 show the results of the buckling analyses of the lipped channel section with a length of 200 mm and ratios of flange to web widths *(b_2/b_1)* varying from 0.00005 to 0.8. The lip size of 20 mm is used throughout the analyses. The corresponding buckling mode shapes are shown in Fig 14.

As can be seen in Fig 13, the value of k_v for *Case A* is 9.973 which is higher than 9.245 of the unlipped channel section in Section 3.3 when the ratio of b_2/b_1 is 0.00005. The value of k_v increases to 11.419 when the ratio of b_2/b_1 reaches 0.1 and then reduces slightly when the ratio of b_2/b_1 keeps increasing to 0.8. The explanation is quite similar to that of Section 3.2. The flanges with lips contribute to the improvement of shear buckling capacity of lipped channel section member and the slenderness of flange width is the reason for the reduction of the value of k_v when the flange width is larger.

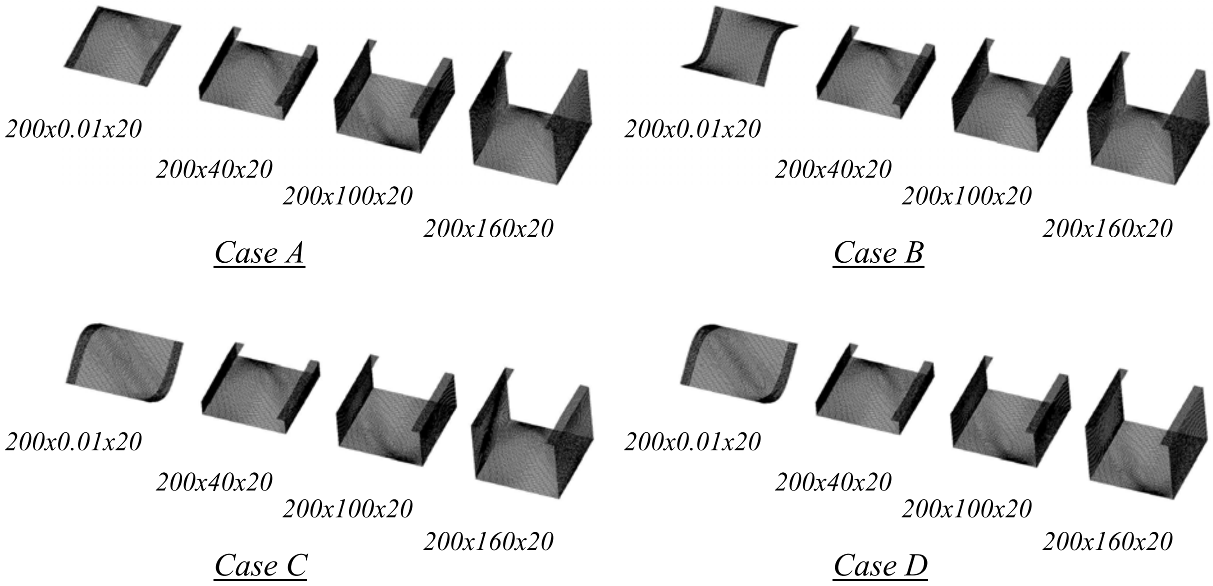

Figure 14. Buckling Mode Shape of Lipped Section – Length = 200 mm, b_2/a = 1.0

It can be seen in Fig 13 that the k_v curves of *Case B* and *Case C* coincide. The values of k_v are 5.208 and 5.516 respectively when the ratio of b_2/b_1 is 0.00005. The values of k_v increase to 11.184 and 11.191 which are close to that of *Case A* as the ratio of b_2/b_1 is 0.1. The values of k_v then reduce slightly and match with that of *Case A*. It is interesting to note that the value of k_v for *Case C* does not reduce as the ratio of b_2/b_1 increases to 0.8 due to pure shear flow in the lip and flange. This fact can be explained that flanges with lips and short member length (L=200 mm) improve considerably the shear buckling capacity of the flanges. The k_v curve of *Case D* is quite similar to that of unlipped channel section in Section 3.3. The value of k_v is higher due to the presence of the lips.

4. CONCLUSION

This report has outlined buckling analysis of channel section members subject to shear stresses. Unlipped and lipped channels were analysed by the Isoparametric Spline Finite Strip Method program. Four different shear flow distribution cases with two boundary conditions are considered in this study. These boundary conditions are simply supported with and without lateral restraints along two longitudinal edges of web panel. Two different member lengths were chosen to investigate the effect of length/width on the shear buckling stresses.

By varying the flange width, the analysis results show that the flanges can have a significant influence on improvement of the shear buckling capacity of thin-walled channel sections. Moreover, it is also demonstrated that the lack of lateral restraint for sections with narrow flanges can lead to premature buckling of the section in a twisting and lateral buckling mode.

REFERENCES

Bleich, H. 1952. “Buckling Strength of Metal Structures”, *McGraw-Hill Book Co. Inc*, New York, N.Y.

Bulson, P. S. 1970. “Stability of Flat Plates”, *Chatto & Windus Ltd.,* London W.C.2.

Cheung, Y. K. 1976. “Finite Strip Method in Structural Analysis”, *Pergamon Press, Inc.*, New York, N.Y.

Eccher, G. 2007. “Isoparametric spline finite strip analysis of perforated thin-walled steel structures”, *PhD Thesis, The University of Sydney, University of Trento,* Australia & Italia.

Lau, S. C. W. and Hancock, G. J. 1986. “Buckling of Thin Flat-Walled Structures by a Spline Finite Strip Method”, *Thin-Walled Structures*, Vol. 4 1986, pp 269-294.

Timoshenko, S. P. and Gere, J. M. 1961. “Theory of Elastic Stability”, *McGraw-Hill Book Co. Inc*, New York, N.Y.